

CFD Analysis of a Formula One Car Model

Introduction

During this investigation, the aerodynamic properties of a Formula One race car are investigated using CFD modelling and simulation. The models are created using OpenFOAM using a provided standard mesh, and making alterations to the program in order to analyze a variety of output parameters. The experiment is most concerned with the effects of different mesh refinements, car speeds, and turbulence models on the various output parameters observed using paraView.

Theory

For the $k - \epsilon$ model, the expected initial values for turbulent energy (k), and viscosity (ν) are calculated using the following equations.

$$k = \frac{3}{2}(U_{Ref}T_i)^2 \quad [\text{Equation 1}]$$

Where T_i is the turbulent intensity (5%), L is the length of the cross section through which inlet flow occurs (.5m), U_{Ref} is the inlet velocity of flow, and ν is the viscosity of the material. The following equation can be used to solve for ϵ .

$$\epsilon = \frac{C_\mu k^{\frac{3}{2}}}{.07L} \quad [\text{Equation 4}]$$

Where C_μ is a given coefficient within the model, and for all calculations will be 0.09. For our $k - \omega$ model, ω can be calculated using the following equation.

$$\omega = \frac{\epsilon}{k} \quad [\text{Equation 5}]$$

Setup/Procedure

An original mesh for the Formula One car is provided and depicted below as the mesh parts of the car are extracted from the mesh block using the Extract Block filter in paraFoam. The mesh was run using the following commands in terminal after the correct initializations were set for each case.

1. blockMesh
2. surfaceFeatureExtract
3. decomposePar
4. mpirun -np4 snappyHexMesh -parallel
5. reconsructParMesh
6. (checkMesh) (erase processors, copy latest timestep polymesh into constant)
7. decomposePar
8. mpirun -np 4 potentialFoam -parallel
9. mpirun -np 4 simpleFoam -parallel
10. reconstructPar
11. paraFoam

The mesh generator snappyHexMesh in OpenFOAM is able to take a pre-created mesh and smoothes the edges as specified in the system. The checkMesh command is not essential to the process but allows for a numerical evaluation of the mesh. The standard model used to run the majority of simulations is the $k - \epsilon$ model, determined in the turbulenceProperties script.

The original, non-refined mesh was tested before using more refined meshes to compare which provided the most optimal results. Meshes were refined by altering (usually increasing) the maximum local cells, maximum global cells, the level ranges of each refinement surface, the level of the features, and the levels of the refinement regions. Additional refinement regions were defined in order to account for the wheels of the car. The refinement process must be carefully executed to increase the cell concentration near the regions of rounded mesh (the wheels and the car) to produce improved results. Coarser, poorly refined meshes create edges where large cells line the border of curves of the model, which lead to increased drag coefficients and inaccurate simulations. The drag coefficients are listed in the log file and are compared for the final timesteps of each simulation. The optimal mesh will then be used to compare results at various velocity values of the car, (as well as incorporated wheel speeds). Surface LIC, velocity vector, pressure, velocity (U_x), and dissipation (turbulent) energy diagrams can also be used to visualize and analyze the different meshes in paraView.

Speeds are altered in the initial conditions U folder and the values for k , ϵ and ω are recalculated given the U value of each simulation. Alterations of the speeds of the wheels can also be achieved in the same U initial condition file under the patches section.

Various turbulence models will be tested as well to observe their effects on the results of the system. An additional script, `RASProperties`, was created in order to outline the turbulence model. The LRR model must be initialized using the $k - \epsilon$ model to bypass a coding bug in the model.

Results/Analysis

Results generated using the original, non refined mesh are used as a reference to help determine the quality of the refined meshes.

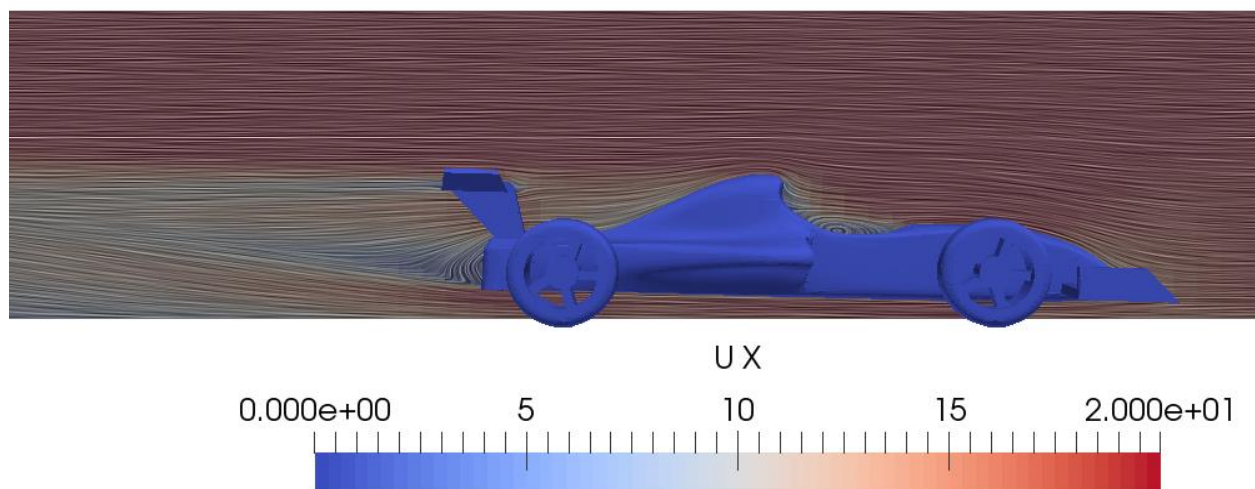


Figure 2. Surface LIC diagram of the back wall with U_x color scheme of non refined model.

[Figure 2] highlights an expected recirculation zone shown in the midsection of the vehicle. [Figure 1] better depicts the pit, the boundaries of which induce recirculation of the airflow. The LIC diagram and x-velocity coloring displays the flow for the middle of the car. Lower velocity patterns behind the car display expected behavior where the car blocks the flow. The LIC patterns also seem realistic in this region, disrupted by the presence of the car.

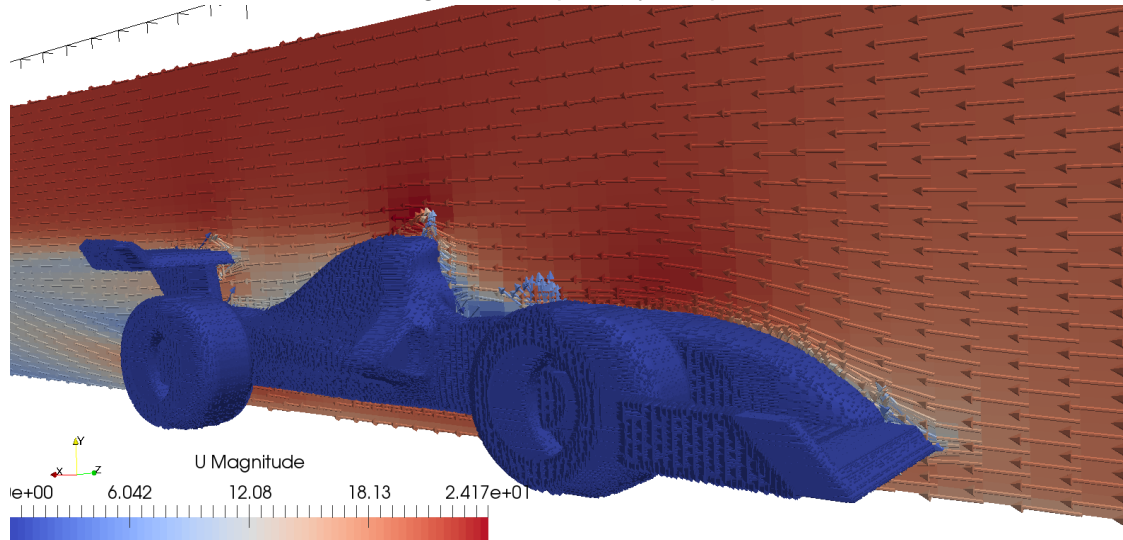


Figure 3. Velocity vector (Glyph) diagram of non-refined model with velocity magnitude coloring

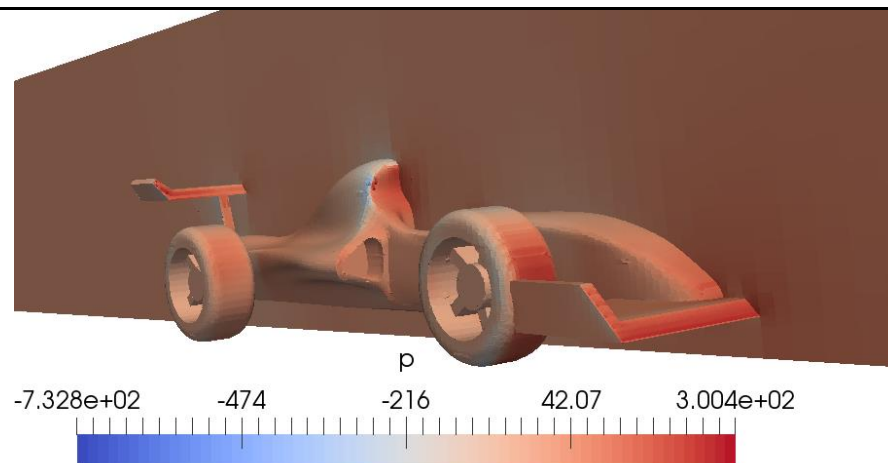


Figure 3. Pressure diagram of car and back wall of non-refined model.

More easily observed under further magnification, the pressure values colored in [Figure 3] include a patch near the edge of the back of the driver's seat. This coloring indicates an edge sticking out from the surface where pressure would build up and possibly a hole in the mesh where the magnitude of negative pressure is extremely high. Apart from this obvious deformity in the mesh, pressure patterns appear realistic. The forward oriented faces of the car display patterns of higher pressure than those displayed by the backwards oriented faces.

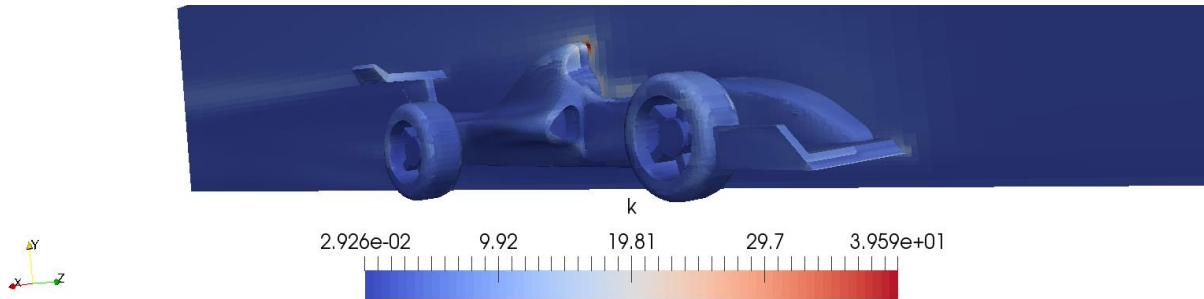


Figure 4. Diagram of the energy dissipated in the non refined model with spinning wheels

Maximum energy dissipation over the back wall of the model is displayed at the top of the driver's seat, as well as the wheels. The energy is dissipating at the greatest rate between surfaces creating contrasting flow to bordering areas. The rotation of the wheels opposes the airflow coming at the car on regions with the higher k values. The top of the car represents the boundary of the recirculation zone at which the direction of recirculation directly opposes the direction of the inlet airflow. Surfaces around the indent also show elevated dissipation values, including the area at which the hole appears to be from [Figure 3]. Diagrams of ϵ displayed constant values on visible all areas of the system at the back wall.

Mesh Refinement Study

A variety of meshes were evaluated to test the result of the refinement on the results of the system.

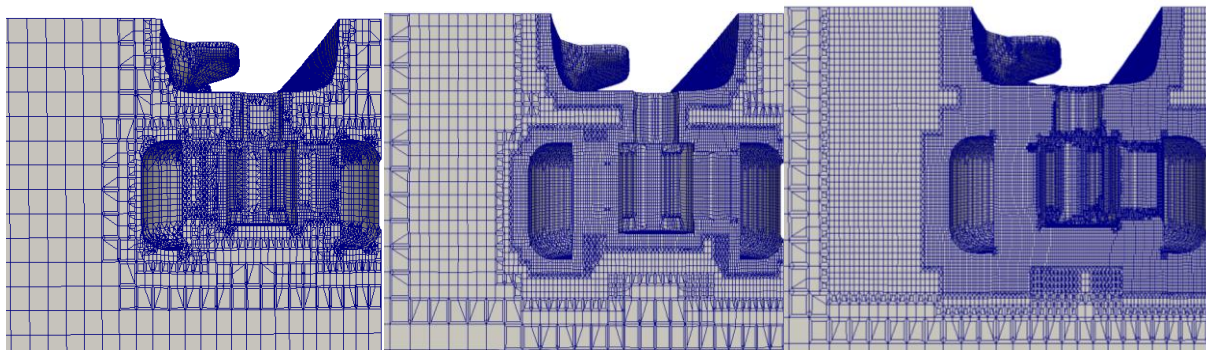


Figure 5. Front wheel cross sections of unrefined (left), refined (middle) and ultra-refined (right) meshes.

The meshes are highlighted at the front wheel area to show a variety of refined or fine meshed surfaces up close. The unrefined mesh shows more specific fine celled mesh due to the fact that the refinements made in snappyHexMesh refined box regions containing the parts of the car instead of the parts themselves. Mesh refining itself rounds the mesh, while the maximum local and global cells allow for more cells to be included in the total or refinement areas. The pictured ultra-refined mesh was refined using 200000 as the global maximum and 1000000 as the global maximum. The pictured refined mesh was refined using 160000 as the global maximum and 600000 as the global maximum.

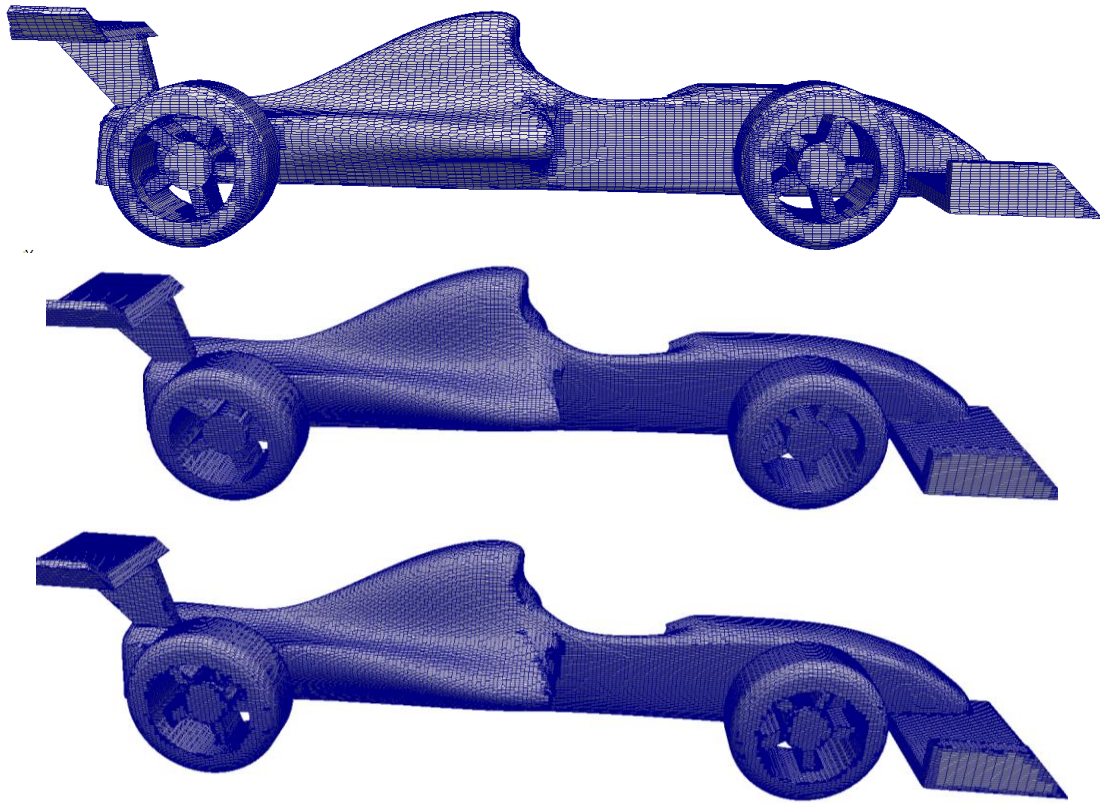
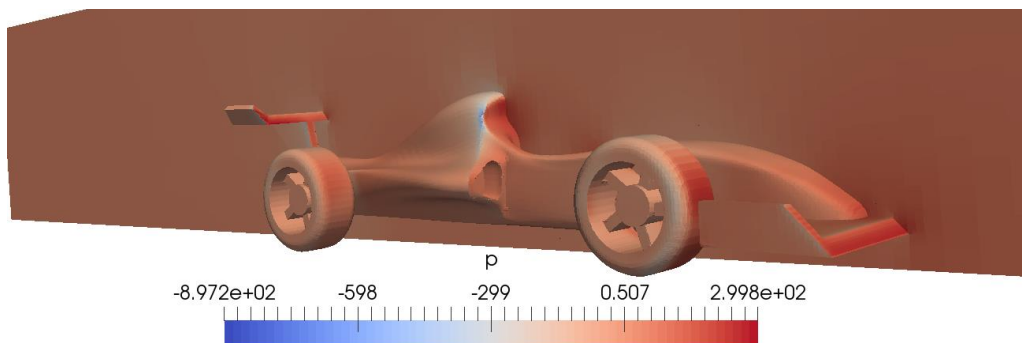


Figure 6. Overall mesh structures of the vehicles for non-refined (top), refined (middle), and ultra-refined (bottom) mesh configurations.

It is clear that the refined meshes have more cells in the bodies of the cars. The pressure and velocity maximum values and diagrams displayed between the non refined and the refined mesh do not differ drastically. Comparing the ultra refined mesh to the non refined mesh however, offers contrast.



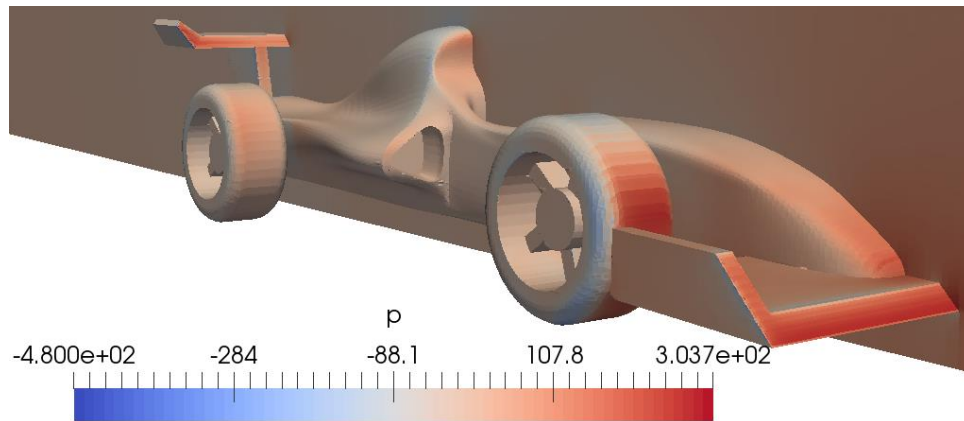


Figure 7. Pressure diagram of refined (top) and ultra-refined (bottom) mesh configuration running at 20 m/s

Referring back to [Figure 3], the disturbance in the surface of the top of the driver's seat has been smoothed out, according to the lack pressure buildup.

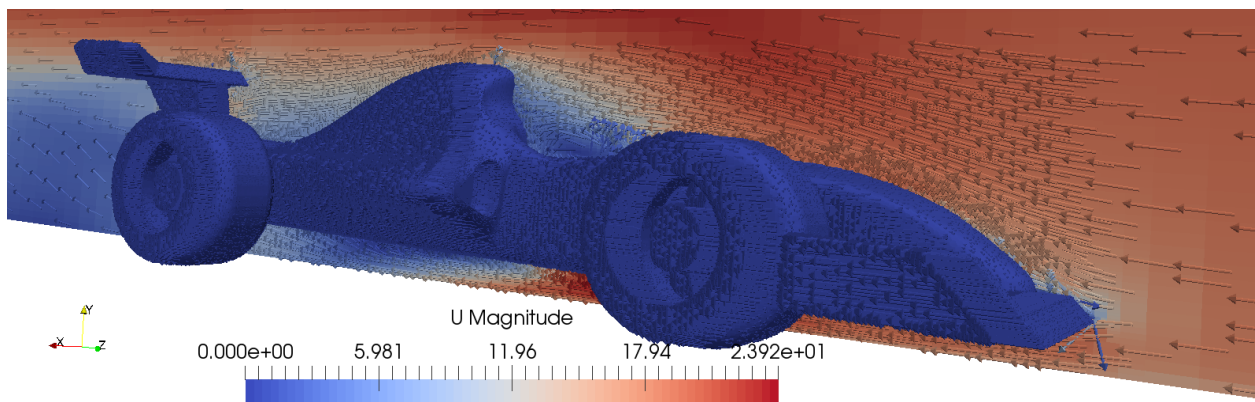
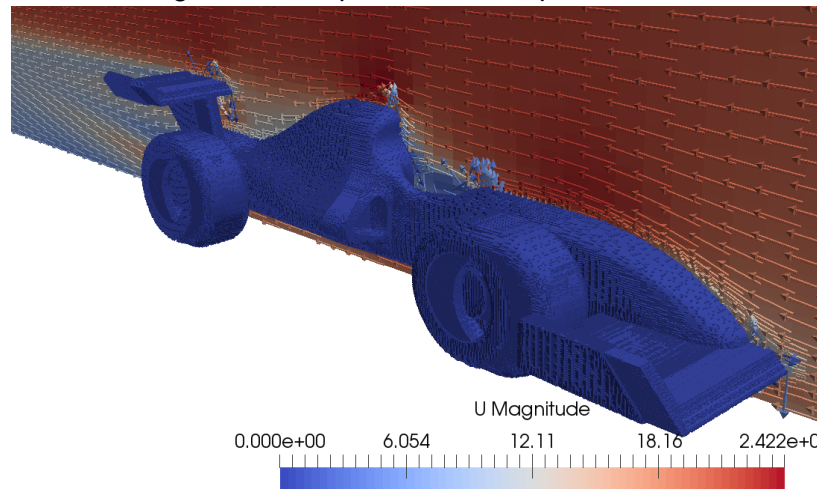


Figure 8. Velocity vector diagrams for refined (top) and ultra-refined (bottom) mesh configuration running at 20 m/s

The refined mesh depicts flares of stray arrows over the top edge of the car indicating meshing problems with skew edges or boundaries sticking out. The region underneath the car in the ultra refined mesh diagram in [Figure 8] shows a recirculation zone paired with a significant loss of velocity. This is an area where the refined mesh borders coarser mesh outside of the refinement region, so there is a possibility that a boundary issue is at play and the mesh is too fine in the refinement regions. The region separations is apparent because of the spacing of the arrows, proportional to the centers of the cells. Upon closer investigation there appears to be a break in the thickly assorted arrows, implying that an area on the back wall of the diagram possesses horizontally coarse mesh. Apart from this deformity, the other features of the ultra fine diagram indicate more accurate results from the smoother mesh with less stray arrows along the top than the other observed configurations

A mesh convergence study was conducted to determine what could be an optimal threshold of the drag coefficient on the vehicle, which will help determine the best mesh to use in the next waves of simulations. Drag coefficients in a recent study estimated typical drag coefficients of a simulated formula 1 vehicle to be between 0.75 and 0.9.

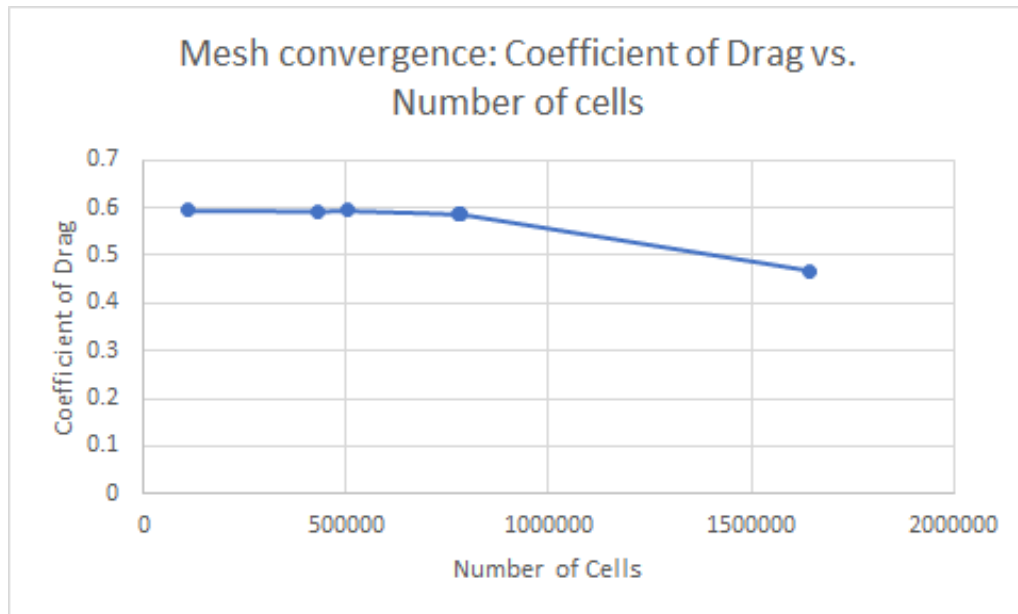


Figure 9. Mesh convergence plot of different refinement configurations. 8 total meshes evaluated, some overlapping closely with others.

The mesh convergence shown in [Figure 5] displays an uneven distribution of cell values due to the inability of the simpleFoam function to converge when running with snappyHexMesh on many combinations of refinement. The areas crowded with data points represent converging refinement properties and variations of these properties with similar configurations, hence the similar number of cells. The coefficient of drag seems to hover around .59 for most mesh configurations with the exception of the ultra-refined mesh. Considering the lack of variation (at 20 m/s). This is outside of the typical range, but because the car is operating at a generally low speed for this type of vehicle, the data makes sense to be below expected values. Although the ultra-fine mesh does seem to be the smoothest and most accurate mesh in most cases, the

time taken to solve this mesh using simpleFoam took a bit less than 2 hours. Due to the time constraints on the experiment, the ultra refined mesh does not make sense to use for comparing other aspects of the simulations. Additionally, observing the mesh convergence as well as the pressure diagrams, the problems presented by the unrefined mesh were not fully solved by the refined meshes, and the coefficients of drag between the refined meshes and the unrefined (excluding the ultra refined) differ by a maximum value of 1.28%. Thenon refined mesh runs and solves far more efficiently than any of the refined meshes, therefore it makes the most logical sense to carry out the other aspects of the experiment using the non-refined mesh.

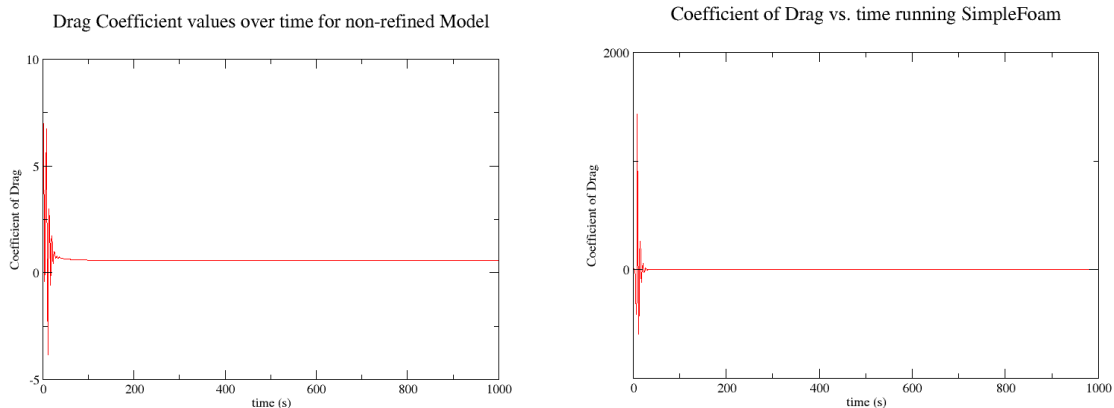
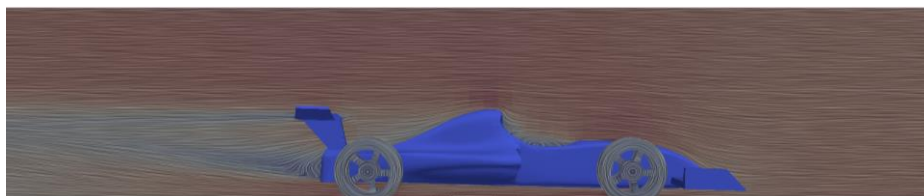


Figure 10. Plots of the Coefficient of drag over time for the non -refined (left) and refined (right) configurations. Y axes values span (-5 10) and (-1000 2000), respectively

Both configuration showed convergence of the coefficient of drag values over the course of time, but the magnitude of the variance of the refined mesh towards the beginning of the trial is significantly greater then the non-refined configuration. This indicates that the mesh solutions solve and converge to realistic values faster using the non refined mesh.

Using the non-refined mesh, the velocity of the vehicle was varied between 30 and 90 m/s in increments of 20, to test at what inlet velocity this configuration operates with the most accuracy. The wheels were also given surface speed, to approximate the tires spinning at a constant angular velocity.



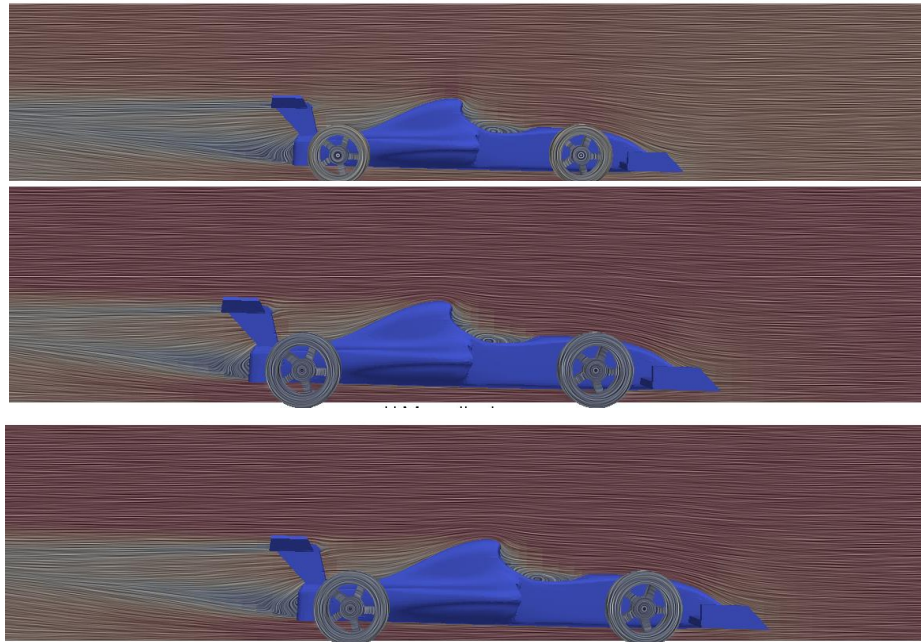
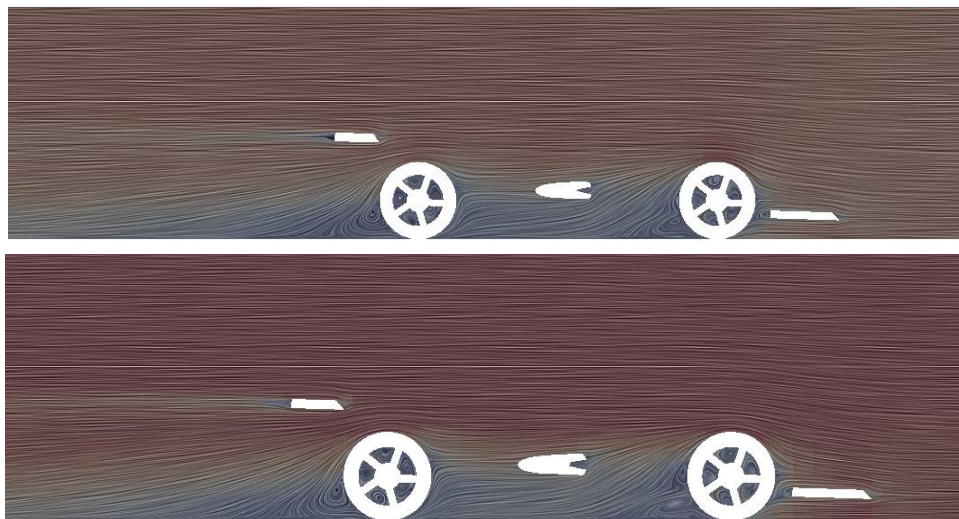


Figure 11. Velocity LIC diagrams for non-refined mesh at velocities of (top to bottom) 30m/s, 50m/s, 70m/s, 90m/s. Maximum magnitude values found in simulation: 36.1m/s, 60.1m/s, 70m/s, and 90m/s.

As the inlet velocities are increased, the region above the car gets darker. This indicates that the velocity of the air rebounding off the surfaces of the car does less to decrease the magnitude around the edges, and ricochets in the positive x direction do not boost the magnitude past the given inlet value. The maximum magnitudes agree, indicating that above a threshold between 50 m/s and 70 m/s the maximum of the magnitude of velocity remains equal to the inlet velocity of the simulation.



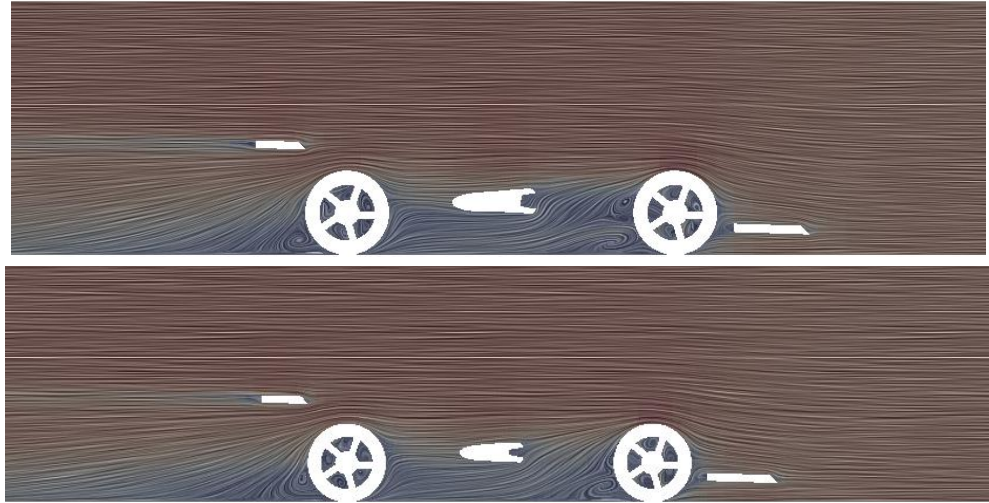


Figure 12. Velocity LIC diagrams at the wheels of non-refined mesh at velocities of (top to bottom) 30m/s, 50m/s, 70m/s, 90m/s. Maximum magnitude values found in simulation: 30m/s, 61.9m/s, 86.6m/s, and 112m/s.

The behavior of the maxima of the maxima of the velocity behave differently across the cross sections of the wheels. In the case of the wheels higher velocity induces higher increases in the maxima from the inlet velocity values. Patterns behind the back wheel at higher speeds return back down more slowly than the slower inlet velocity configuration data. All inlet velocity configuration diagrams display recirculation zones within the spokes of the wheels.

The drag coefficients corresponding to each inlet velocity value are recorded and compared.

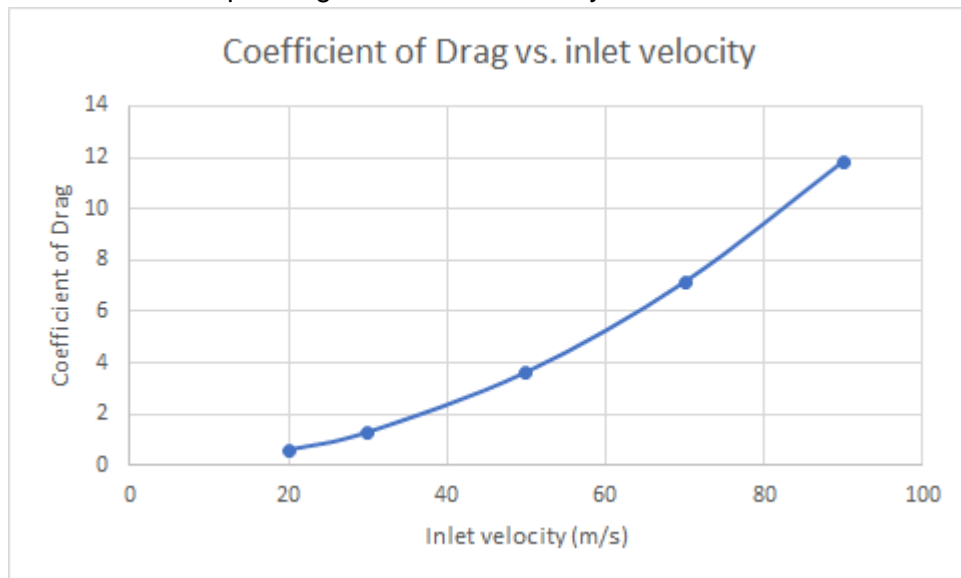


Figure 13. Plot highlighting the relationship between drag and inlet velocity on the non-refined configuration. Drag coefficient for 20 m/s was corrected to that determined with the wheels spinning, from mesh refinement value.

As expected, the coefficient of drag increases as the inlet velocity on the system increases. The coefficient of drag is expected around the 0.75 to 0.9 range. The drag coefficient increases t an unreasonable amount past the inlet velocity value of 50 m/s. The non-refined mesh would likely produce higher drag coefficients than a real-life model so the velocity at which the system produces the most accurate data should be roughly between 20 m/s and 30 m/s. Interestingly, the coefficient of drag decreased when the rotational velocity was added to the wheels.

The model was run using different turbulence Models, determined by the RASModel listed in turbulenceProperties, and results were compared between models.

Model	Maximum Velocity (m/s)	Maximum pressure (Pa)	Maximum Dissipation Energy (J/kg)	Coefficient of Drag
K - ϵ	32.51	294.7	39.72	0.5710
K - ω	20.00	264.4	16.25	0.5262
RNG k - ϵ	24.44	285.9	14.61	0.5439

Figure 14. Table comparing the results of the various models over the specified parameters at 20 m/s inlet velocity.

All parameters in [Figure 14] indicate that the k - ϵ model produced the most basic and inflated results. The model's range of boundary condition refinement along with the presence of and ω parameter likely differed the results of the models. The diagrams of the models did not display different or unusual behaviors, which should indicate that the non-refined mesh was not affected significantly by the change in the models. More refined meshes contain more cells in refinement regions, so it is probable that the refined meshes would see more significant improvements in performance under models that perform better at boundary lines. All models besides k- ω generate values for maximum velocity greater than the inlet velocity, indicating the correction of the model based on ω values generated by the flux from potentialFoam.

Conclusion

The various configurations of refinement were used to determine that significant improvement of the quality of the mesh could not be achieved without major sacrifice in the efficiency of the solvers of the model. SnappyHexMesh operates under very strict and sensitive conditions, with a high risk of failed simulations when refining manually. The non-refined mesh was used to then compare simulations containing variations in the inlet velocities, and the turbulence models used to conduct the simulations. Results for all comparisons displayed a moderate range of performance levels while the different aspects were varied.